Available online at www.iseec2012.com

I-SEEC 2012

Proceeding - Science and Engineering (2013) 252–257

Proceeding
Science and Engineering

www.iseec2012.com

Science and Engineering Symposium
4th International Science, Social Science, Engineering and Energy Conference 2012

Neutral-Point-Clamped Multilevel Inverter Using Space Vector Modulation for Three-phase Induction Motor

A. Charean[a,*], W. Sawaengsinkasikit[a], N. Koetsam-Ang[a], V. Tipsuwanporn[b]

[a]Department of Electrical Engineering, Faculty of Engineering, Kasem Bundit University, Bangkok, 10250, Thailand
[b]Department of Instrument and Control Engineering, Faculty of Engineering,
King Mongkut's Institute of Technology Ladkrabang, Bangkok, 10520, Thailand

Abstract

Neutral-Point-Clamped Multilevel Inverter with Space Vector Modulation (NPCSV) is important in implementing in the industry of driving system, high-voltage system, and system which requires high efficiency. This paper proposes a new method for driving 3-phase induction motor with three-level voltage inverter. The three-level voltage inverter has many switching conditions compared to two-level voltage inverter. In order to simplify the use of three-level inverter as the use of two-level inverter, such proposed method can be applied to any multi-level inverters. In this paper, Space Vector Modulation is implemented to construct the three-level inverter for the three-phase induction motor. Results obtained from experimentation show that current signal was more like a sine-wave form than the signal from the two-level inverter and could be used to drive actual induction motor.

Keywords: Neutral-Point-Camped Multilevel Inverter, Space Vector and PWM.

1. Introduction

Currently, the development of power electronics and semi-conductor technology is growing, so different multi-level inverter circuits are more interesting to research [1-2]. Nowadays, three-level voltage-fed PWM inverter has been used popularly for many million kilowatts in the industry [3]. The main reason for this is that the output voltage signals from the multi-level inverter have low switching frequency resulting to high efficiency, low deviation signal, and provide high voltage between the seriesed devices. Recently, the Space vector PWM technique has become a popular technique and more interesting. Results of such technique provide higher output voltage at the main frequency when it is compared to the sinusoidal PWM. One of the benefits of the multi-level inverter is reduction of voltage stress on each switch. Furthermore, characteristics of the signal have low harmonics comparing to the two-level signals at the same switching frequency. However, the structure of

* Corresponding author.*E-mail address:* acharean@yahoo.com

SVPWM used in the three-level inverter is more complex because of many switching status. In this paper, the multi-level inverter was designed with diode-clamped and tested to drive 0.4-kW motor (1/2 hp). Such multi-level inverter was easily utilized to increase the voltage level for higher voltage applications with low THD and low switching frequency. Such characteristics are very difficult to be available in the general two-level inverter.

2. Generation of Space Vector PWM Signal for Three level Inverter

Figure 1 shows circuit of Neutral-Point-Clamped, multi-level inverter by separating dc supplier. Three-phase output voltage signals are generated by switching at each transistor. The obtained signals are +Ud/2, 0, and -Ud/2.[4]

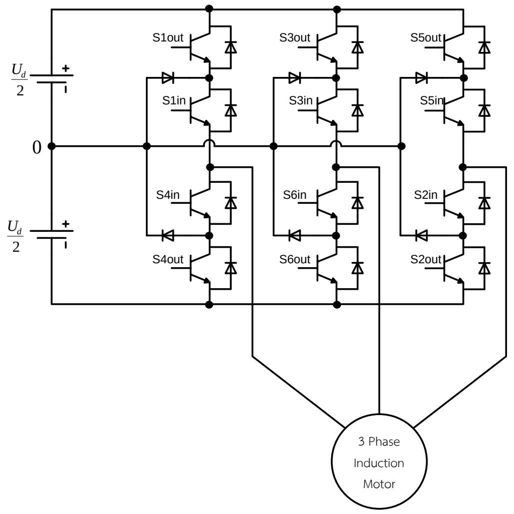

Fig. 1. Neutral-Point-Clamped, Multi-level Inverter Circuit

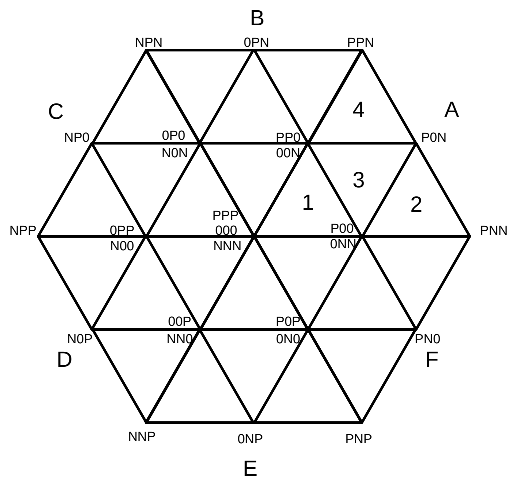

Fig. 2. Space Vector Diagram of Three-level Inverter

Switching of the three-level inverter can be divided into 3^3= 27 patterns, and space vector diagram of the three-level inverter can be divided into 6 sectors (A, B, C, D, E, and F), as shown in Figure 2, which have 24 varying voltage patterns and 3 zero voltage patterns at the central position of the hexagon. Each sector can be separated to 4 areas (1, 2, 3, and 4). The switching patterns of the inverter for phase A are demonstrated in Table 1. [5]

Table 1. Switching Patterns of the Inverter for Phase A

Voltage Level of Van	Switch "On"
-Ud/2	S4in, S4out
0	S4in, S1in
Ud/2	S1in, S1out

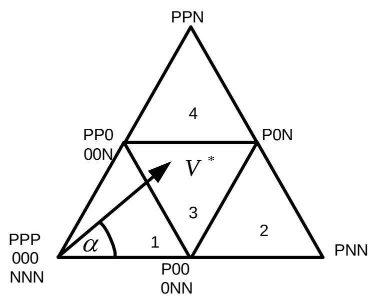

Fig. 3. Sector A and Switching Conditions for Three-level Inverter

According to principle of SVPWM, the required voltage vector is calculated approximately by using three adjacent vectors. The period employed by each voltage vector can be calculated by

$$T_1V_1 + T_2V_2 + T_3V_3 = T_sV^* \tag{1}$$

$$T_1 + T_2 + T_3 = T_s$$

While V_1, V_2 and V_3 are vectors determining the boundary of triangular vector V^* (Command Vector) in the area. T_1, T_2 and T_3 are similar time vectors and T_s is random time. The three-level inverter is similar to the two-level inverter that has its individual space vector diagram divided into 6 sectors. The determination of switching pattern and technique of each sector are analogous. For the reason of convenient, only the switching patterns of sector A is explained to understand. Sector A is divided into 4 boundaries as shown in Figure 3 and demonstrates all available switching patterns. SVPWM for the three-level inverter can be implemented by using sequence of decision vectors, selection of sector boundary, calculation of switching time T_a, T_b, T_c, and determination of switching conditions.

2.1. Determination of Sector

Value of α is calculated and position of the sector of command vector V^* can be determined as follow:

If α is $0 \le \alpha < 60°$, then V^* is in sector A
If α is $60 \le \alpha < 120°$, then V^* is in sector B
If α is $120 \le \alpha < 180°$, then V^* is in sector C
If α is $180 \le \alpha < 240°$, then V^* is in sector D
If α is $240 \le \alpha < 300°$, then V^* is in sector E
If α is $300 \le \alpha < 360°$, then V^* is in sector F

2.2. Determination of Sector Boundary

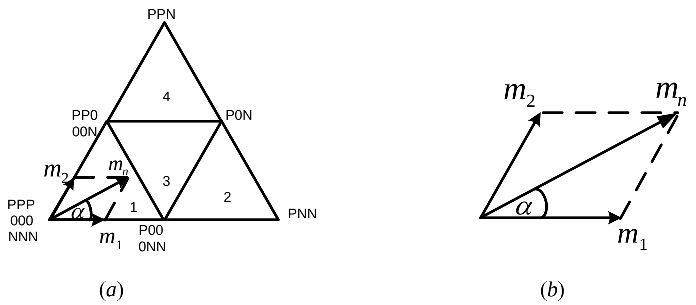

Fig. 4. Space Vector Diagram for m1 and m2 in Sector A

According to Figure 4(b), m_1 and m_2 can be calculated as follow:

$$a = m_2 = \frac{b}{\sin(\pi/3)} = \frac{2}{\sqrt{3}}b = \frac{2}{\sqrt{3}} \cdot m_n \cdot \sin\alpha \tag{2}$$

$$m_1 = m_n \cdot \cos\alpha - \left(\frac{2}{\sqrt{3}} \cdot m_n \cdot \sin\alpha\right)\cos(\pi/3) \tag{3}$$

$$m_1 = m_n\left(\cos\alpha - \frac{\sin\alpha}{\sqrt{3}}\right) \tag{4}$$

If m_1, m_2 and $(m_1 + m_2) < 0.5$, then V^* is in the 1st boundary
If $m_1 > 0.5$ then V^* is in the 2nd boundary
If m_1 and $m_2 < 0.5$ and $(m_1 + m_2) > 0.5$ then V^* is in the 3rd boundary
If $m_2 > 0.5$ then V^* is in the 4th boundary

2.3. Determination of Switching Conditions

By considering to switching transmission in each of equipment at different time, the sequence of switching for each boundary in the sector A is demonstrated below. If all of the switching conditions in each boundary are used, the switching signal of the sector A will be:

1st boundary: NNN, 0NN, 00N, 000, P00, PP0, PPP
2nd boundary: 0NN, PNN, P0N, P00
3rd boundary: 0NN, 00N, P0N, P00, PP0
4th boundary: 00N, P0N, PPN, PP0

3. Experimentation Results

In this research, testing was performed by the use of a 3-phase induction motor (rated 380 Volt, 0.4-kW (1/2 hp), and 1410 rpm) with star-type connection. Figure 5(a)-(b) demonstrates testing results of the two-level inverter at frequency of 20 and 50 Hz by setting the modulate index equal to 0.4. The 1st, 2nd, and 3rd channels demonstrate voltage signal of phase A, B, and C respectively. The current signal at phase A are shown in the 4th channel by setting the channel magnitude to 100 mV per 1 ampere current. Figure 6(a)-(b) demonstrates testing results of the NPCSV inverter at frequency of 20 and 50 Hz by setting the modulate index equal to 0.4.

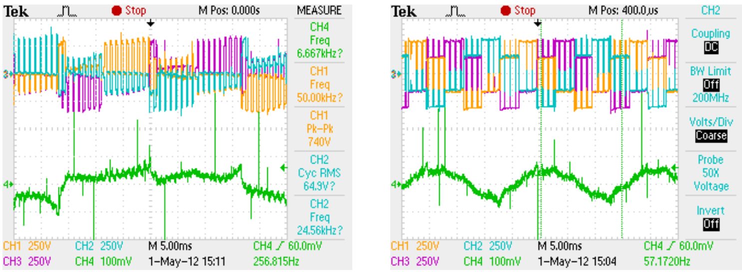

(a) (b)

Fig. 5. Voltage and Current Signal of Two-level Inverter at Frequency of 20 and 50 Hz for m =0.4

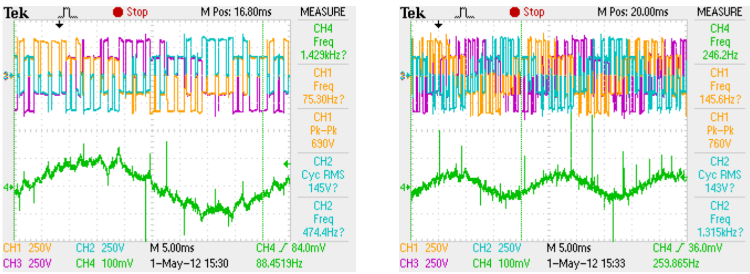

(a) (b)

Fig. 6. Voltage and Current Signal of NPCSV Inverter at Frequency of 20 and 50 Hz for m =0.4

Voltage and current signals of the NPCSV inverter are illustrated in Figure 7(a) where the 1st, 2nd, and 3rd channels demonstrate the voltage signal of phase A, B, and C respectively. Figure 7(b), the 1st, 2nd, and 3rd channels demonstrate the current signals of phase A, B, and C by setting the channel magnitude to 1000 mV per 1 ampere current at 20 Hz.

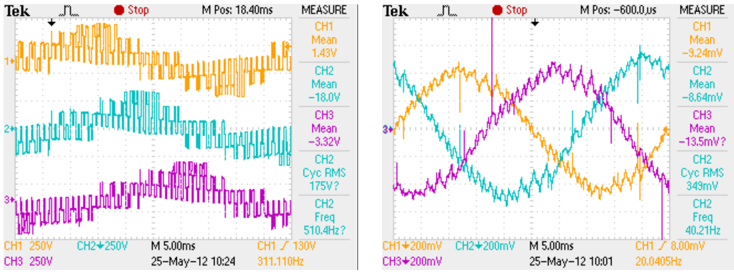

(a) (b)

Fig. 7. Voltage and Current Signal of NPCSV Inverter at Frequency of 20 Hz for m =0.8

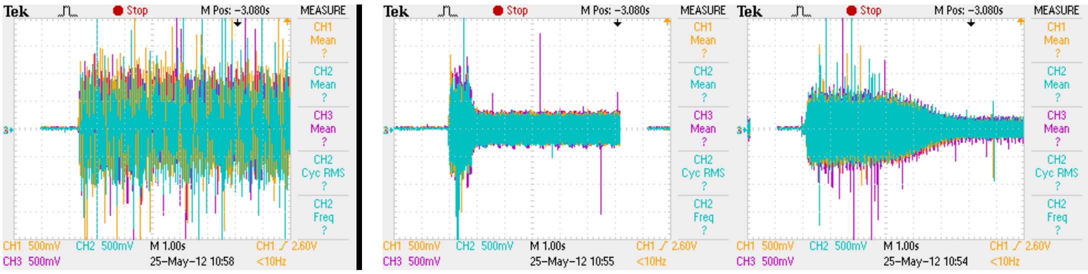

(a) (b) (c)

Fig. 8. Three-phase Current Signal of NPCSV Inverter during Starting the Motor at Frequency of 20, 40, and 50 Hz for m =0.8

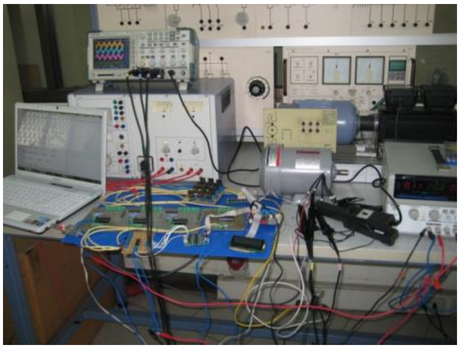

Fig. 9. Testing Equipment of NPCSV Inverter

Figure 8 (a)-(c) demonstrate the current signal of phase A, B, and C during the 3-phase induction motor is started of frequency 20, 40, and 50 Hz, respectively, by setting the channel magnitude to 1000 mV per 1 ampere current. Figure 9 demonstrates the testing of the 3-phase induction motor drive with the NPCSV inverter.

4. Conclusion

Result from the testing of 0.4-kW (1/2 hp), 3-phase induction motor has shown that the current and voltage signals derived from the NPCSV inverter were more like sinusoidal signal than the two-level inverter. And such proposed multi-level inverter could easily increase the voltage level for high voltage applications with low THD and low switching frequency. These characteristics were very difficult to be made available in the general two-level inverter. It is implied that the research has to be developed to control the 3-phase induction motor by employing the principle of vector in order to increase efficiency.

References

[1] P.M. Bhagwat and V.R. Stefanovic. Generalized Structure of A Multilevel Inverter. IEEE Trans on I.A.,Vol.19,no.6, 1983,pp. 1057-1069.

[2] S.K. Mondal, J.O.P Pinto, B.K. Bose. A Neural-Network-Based Space Vector PWM Controller for a Three-Level Voltage-Fed Inverter Induction Motor Drive. IEEE Trans on I.A.,Vol.38,no.3, 2002,pp. 660-669.

[3] S.K. Mondal, B.K. Bose, V. Oleschuk and J.O.P Pinto. Space Vector Pulse Width Modulation of Three-Level Voltag Extending Operation Into Overmodulation Region. IEEE Trans on Power Electronics. Vol.18,no.2, 2003,pp. 604-611.

[4] A. Nabae, I. Takahashi and H. Akagi. A New Neutral-Point-Clamped PWM Inverter. IEEE Trans on I.A.,Vol.17,no.5, 1981,pp.518-523.

[5] Yo-Han Lee, Burn-Seok Suh, Chang-Ho Choi, Dong-Seok Hyun. A New Neutral Point Current Control for a 3-level Converter/Inverter Pair System. IEEE Trans on I.A.,Vol.3, 1999,pp.1528-1534.